

Full paper

Reconfigurable magnetic soft robots with multimodal locomotion



Yuwei Ju ^{a,b,1}, Run Hu ^{c,1}, Yan Xie ^{a,b,1}, Jianpeng Yao ^{a,b}, Xiaoxiang Li ^{a,b}, Yiliang Lv ^{a,b}, Xiaotao Han ^{a,b}, Quanliang Cao ^{a,b,*}, Liang Li ^{a,b,*}

^a Wuhan National High Magnetic Field Center, Huazhong University of Science and Technology, Wuhan 430074, China

^b State Key Laboratory of Advanced Electromagnetic Engineering and Technology, Huazhong University of Science and Technology, Wuhan 430074, China

^c State Key Laboratory of Coal Combustion, School of Energy and Power Engineering, Huazhong University of Science and Technology, Wuhan 430074, China

ARTICLE INFO

Keywords:
Soft robotics
Magnetic soft robots
Magnetization
Pulsed magnetic field
Deformation
Multimodal locomotion

ABSTRACT

Magnetic soft robots have recently attracted increasing attention owing to their remarkable advantages and potential applications, but the reconfigurable magnetization inside soft-composite materials remains challenging, otherwise they can only achieve fixed magnetic response under external magnetic fields with limited morphological features and motion modes. To tackle this issue, a direct magnetization method based on pulsed high magnetic field focusing is developed, where the local magnetization distribution can be programmed flexibly and reconfigurably after fabrication within milliseconds and millimeter-scale resolution. Based on this method, reconfigurable magnetic soft robots are developed with superior merits, including a fishing soft robot to resist the dynamic drag, an inchworm-inspired crawling robot with a speed more than 1 body/s, and a six-arm rolling soft robot to transport objects in complex environments. The underlying locomotion mechanisms of these soft robots are also well discussed. The developed magnetic soft robots, together with the proposed magnetization method, are expected to pave avenues for the future development of mass production and controllable magnetization of soft robots for practical applications.

1. Introduction

Soft robots, due to their abundant advantages in terms of scalability, flexibility, and adaptability, have garnered increasing attentions for potential applications in biomedical, bioengineering, bionics, automation, and industry [1–4]. With the development of soft-composite materials and flexible actuation technologies, soft robots have become a large branch of robotics discipline, and enabled multimodal locomotion [5–7] and applications in unstructured environments [8–10]. Up to now, a variety of actuation methods have been used to manipulate soft robots, such as pneumatic pressure [11,12], electrical fields [13–15], magnetic fields [6,16–21], and light [7,22,23]. Among these methods, the magnetic actuation holds the most promise in three aspects [24,25]: 1) non-contact and useful in combination with untethered control; 2) easy to penetrate most materials (non-magnetic or weakly magnetic materials) and safe for living organisms due to low-strength actuation methods (less than 0.5T), which is of special interest for biomedical application; 3) agile to generate static and dynamic magnetic fields via current-controlled electromagnets or motion-controlled permanent

magnets, offering precise and flexible actuation strategies. As a result, multi-scale soft robots based on magnetic actuation have received increasing attention [26]. To achieve magnetic soft robots, it is a general strategy to embed hard magnetic particles into soft materials [27], and regulate their magnetic alignment directions by specific magnetization methods, like assembly-type magnetizing [28–30], template-aided magnetizing [6,31,32], and magnetic field-aided re-orientation of magnetized particles [33–35]. The last magnetization strategy is the most promising in term of high precision and flexible magnetizing, which can be implemented via 3D printing [33], ultraviolet (UV) lithography [34] and heating [35]. Nevertheless, these magnetization progresses typically do not perform well in terms of reconfiguration capability. As mentioned by Alapan et al. [35], the magnetization profiles of soft robots produced by 3D printing and lithography-based programming can no longer be reprogrammed as the magnetic programming process is finished almost simultaneously with the fabrication process. The heating-based programming method can solve this problem, while its suitability is limited to thin-walled robots due to the limited penetration depth of the laser heating. In addition, Song et al.

* Corresponding authors at: Wuhan National High Magnetic Field Center, Huazhong University of Science and Technology, Wuhan 430074, China

E-mail addresses: quanliangcao@hust.edu.cn (Q. Cao), Liangli44@hust.edu.cn (L. Li).

¹ These authors contributed equally to this work.

[16] demonstrated that the magnetization profile of soft magnetic composite materials can be reprogrammed by solid liquid phase transition of polymer encapsulating the ferromagnetic particles, while the used magnetization process of this method is similar to the template-aided magnetizing process and requires an additional heating process.

Here, reconfigurable magnetic soft robots with multimodal locomotion are reported, where a simple direct magnetization method is developed to alter internal magnetization profiles in the soft robots with millimeter-scale resolution. Our method holds merits like controllable and directional magnetization, reconfigurable magnetization, and enables multimodal locomotion, which cannot be achieved by the conventional unidirectional magnetization systems without any assistance

[28–32]. Multi-dimensional deformations of magnetic soft robots with designed magnetization profiles are demonstrated both numerically and experimentally, with revealing the underlying mechanisms. Furthermore, several magnetic soft robots are developed and new magnetic actuation strategies are proposed to achieve multimodal locomotion in dynamic magnetic fields.

2. Results and discussion

2.1. Reconfigurable magnetization method and its application in magnetic soft robots with radial magnetization

Fig. 1A shows the working principle of the proposed direct

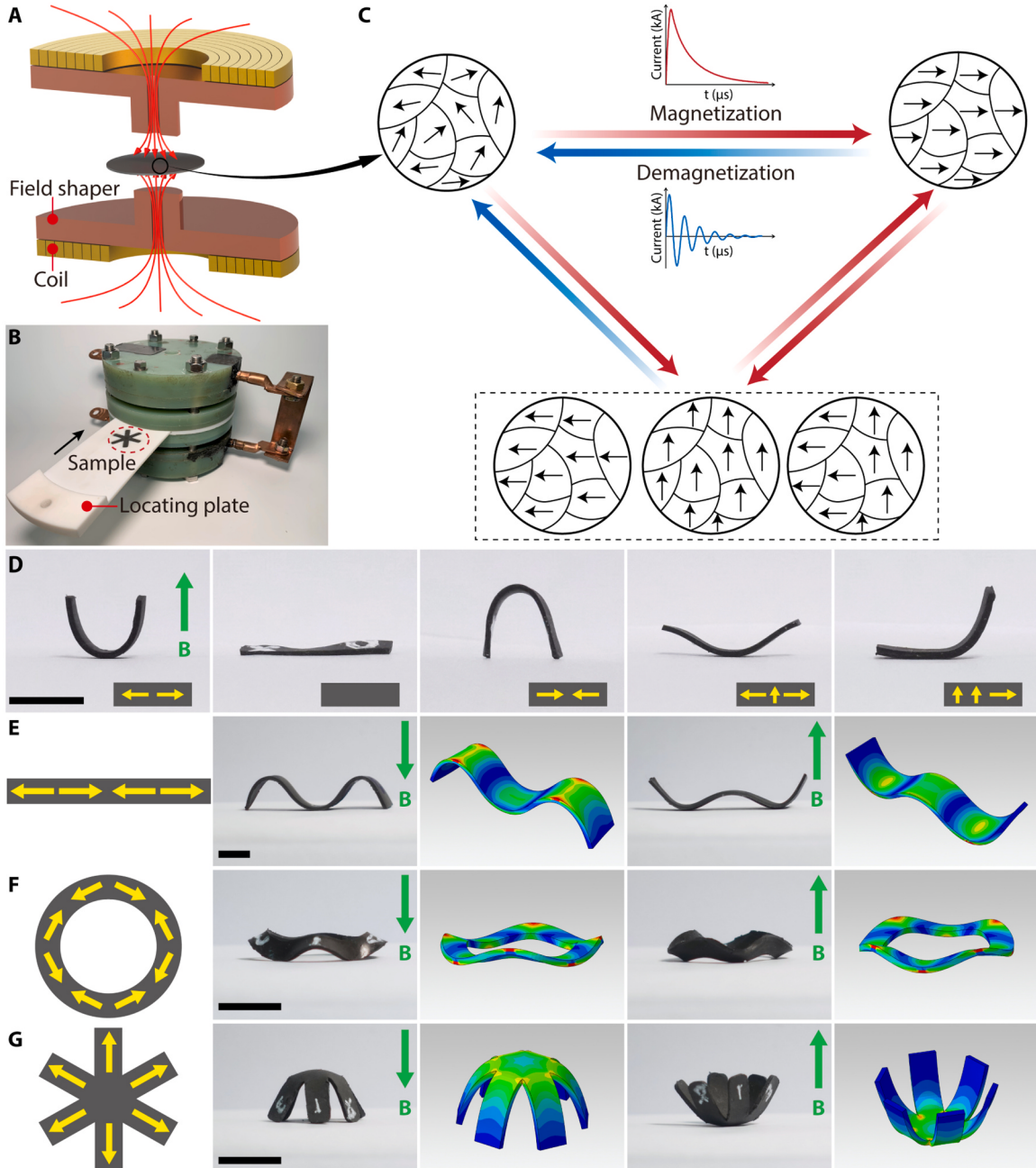


Fig. 1. Reconfigurable magnetization process and multimodal shape transformation. (A) Schematic of the magnetization process. (B) The dual-coil setup. (C) Schematic principle of the reconfigurable magnetization process. (D) Experimental demonstration of the reconfigurable magnetization. Experimental and numerical demonstration of diverse magnetization patterns and complex deformed shapes under a magnetic field of 7 mT: (E) strip-like robot, (F) circular-like robot, (G) multi-arm robot. Green and yellow arrows represent the magnetic field direction and the magnetization direction, respectively. Scale bar: 10 mm.

magnetization system. A dual-coil system with field shapers is proposed to generate pulsed high magnetic fields for magnetization. Different with conventional direct magnetization systems, the designed field shapers can concentrate the high magnetic fields to a small scale within a few millimeters for local controllable magnetization (Figs. S1 and S2). Fig. 1B shows the photograph of the dual-coil setup. The detailed design and working principle of the magnetization system are presented in Text S1 in the Electronic Supplementary Information. Fig. 1C illustrates the reconfigurable magnetization process for magnetic soft robots. Both oscillating and non-oscillating pulsed magnetic fields can be generated in the proposed magnetization system (Figs. S3A and S4), which are used for magnetization and demagnetization process, respectively. This allows the local magnetization of the samples to switch between nonzero and zero state. Meanwhile, the magnetic field direction in the sample region can be flexibly controlled by adjusting the direction of currents flow in the two coils, where both radial and axial magnetic fields for multi-directional magnetization can be achieved (Fig. S3B and Fig. S3C). Importantly, the inner magnetization direction in the samples after their fabrication process can be reoriented by non-oscillating discharges, which serves as the basis for the reconfigurable magnetization. For instance, as shown in Fig. 1D, the proposed magnetization system is able to achieve: 1) demagnetizing of a preset magnetic soft robot, 2) adding an additional vertical magnetization component, and 3) reversing or partially changing the previous magnetization profile, thus enable different deformation morphologies under the same magnetic field. In addition, more diverse magnetization distributions and complex deformed shapes can be achieved, using progressive loading (i.e. multi-step magnetization). For instance, a new type of magnetization can be realized in a 1D strip, based on a two-step loading magnetization mode, by adjusting the relative position between the soft robot and the field shaper. The "m"- and "w"-like shapes can be obtained by applying downward and upward magnetic fields, respectively (Fig. 1E). Similarly, we can obtain 3D ring-like shapes with alternating arches based on a

four-step loading magnetization method (Fig. 1F). Due to the symmetric magnetic field generated by the proposed magnetization system, the magnetization pattern shown in Fig. 1G can be easily achieved using only a single discharge within milliseconds, which is very suitable for high-throughput development of multi-arm magnetic soft robots. 3D numerical simulations of the above-mentioned robots under magnetic fields are also carried out in Fig. 1E-G, from which the deformation morphologies of these soft robots agree with the experiment and validate our design clearly. The dynamic locomotion process of these robots in numerical simulation and experiment can be seen in Movie S1.

Supplementary material related to this article can be found online at doi:10.1016/j.nanoen.2021.106169.

2.2. Magnetic soft robots combining radial and axial magnetization

The magnetic response of soft robots under radial and axial magnetization are significantly different. Therefore, the combination of the two-magnetization modes could enable more dynamic characteristics of magnetic soft robots. As schematically shown in Fig. 2A, when an external magnetic field (green dashed lines) orthogonal to the initial magnetization is applied, the magnetic moment \mathbf{m} (red arrows) tends to align with the external field under a magnetic torque τ_m in the radial magnetization mode (mode 1). The magnetic moment deflects to \mathbf{m}' when an equilibrium state is reached under the action of multiple factors, such as magnetic torque, gravity, surface static friction and elastic deformation resistance. In this case, when a uniform magnetic field of 15 mT along the negative z-axis is applied, a deformation with amplitude of h_1 can be realized, defined as the vertical distance between the peak point and the ground (Fig. 2B). When an additional negative axial magnetization is superimposed in the central region of the robot (mode 2), the deformation of the soft robot will be determined by the combination of the magnetic torques induced by the radial and axial magnetization components. Fig. 2C shows that the deformation amplitude h_2

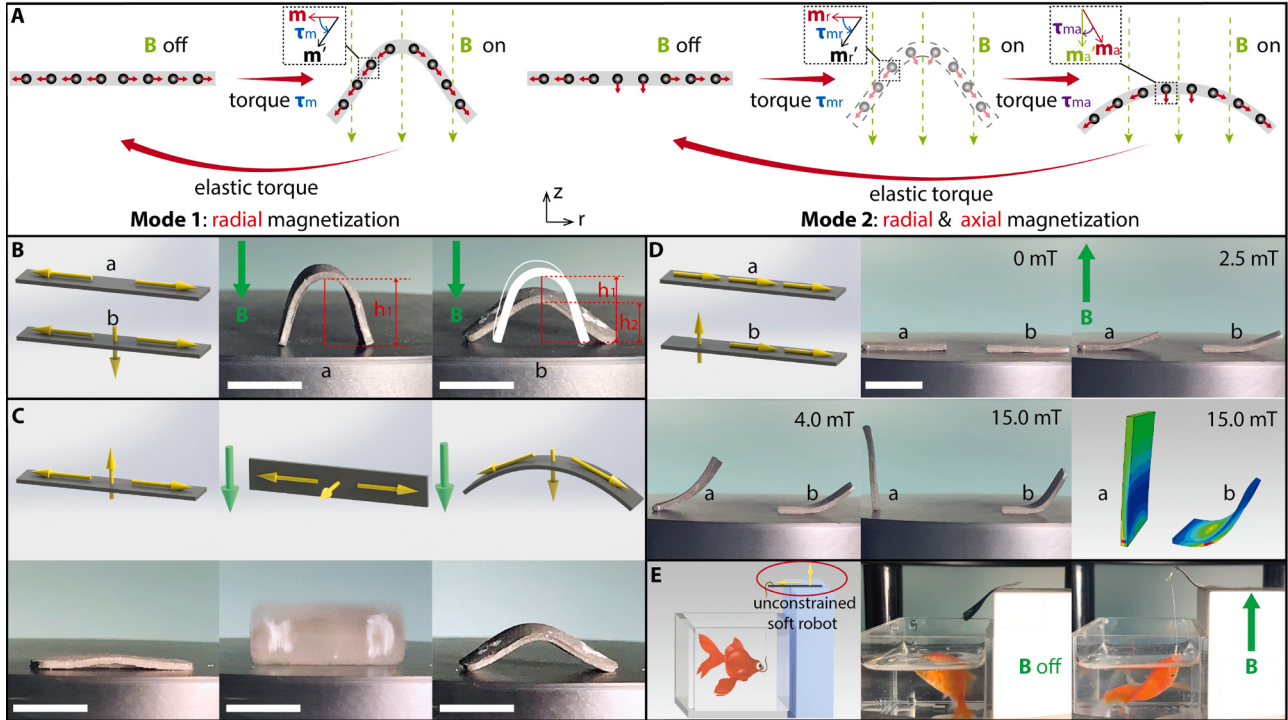


Fig. 2. Deformation behavior of soft robots by combining radial and axial magnetization. (A) Deformation mechanism of soft robots in the radial magnetization (Mode 1) and the superimposed radial-axial magnetization (Mode 2). (B) Robot deformation with two magnetization modes. (C) Robot deformation with magnetization Mode 2, where the initial magnetization direction in the central region is opposite to the magnetic field direction. (D) Demonstration of the deformation behavior of soft robots with a single-direction radial magnetization and a bi-directional magnetization (axial-radial). (E) Application of a magnetic soft robot with a bi-directional magnetization for a simulated fishing scene. Scale bar: 10 mm.

(mode 2) is considerably smaller than h_1 , which is due to the fact that the robot deformation induced by the radial magnetization was suppressed partially by the axial magnetization aligning with the direction of the actuating magnetic field.

The introduction of the additional axial magnetization could bring some unique advantages. For instance, when the direction of the initial axial magnetization is opposite to the external magnetic field direction, the soft robot will flip under the action of the magnetic torque in the center region before an obvious deformation occurs (Fig. 2C). The same deformation process as in Fig. 2B will then occur. This phenomenon indicates that regardless of the initial placement state of the soft robot, the relative positional relationship of two surfaces of the robot after deformation will remain unchanged (Fig. 2C). In other words, the axial magnetization gives the robot the directional selectivity of surface under

magnetic fields. Furthermore, we demonstrate the potential of axial magnetization for the realization of the blank holding function, which can ensure that the soft robot is partially fixed in the deformation process. The soft robot *a* with a single-direction radial magnetization in Fig. 2D can fully stand up to align its magnetization with the direction of the external axial magnetic field, as the magnetic field increases (Fig. 2D). In contrast, for the soft robot *b* with a dual-axis magnetization direction in Fig. 2D, its right part tends to deform along the magnetic field direction, while its left side remains un-deformed which seems to be adhered. This function enables the soft robot to maintain local stability through self-restraint instead of external fixing measures (such as glue fixation) when performing deformation. To further demonstrate its dynamic stability, we present a simulated fishing scene, where a soft robot with a weight of 0.167 g acts as a fishing pole (Fig. 2E). When no

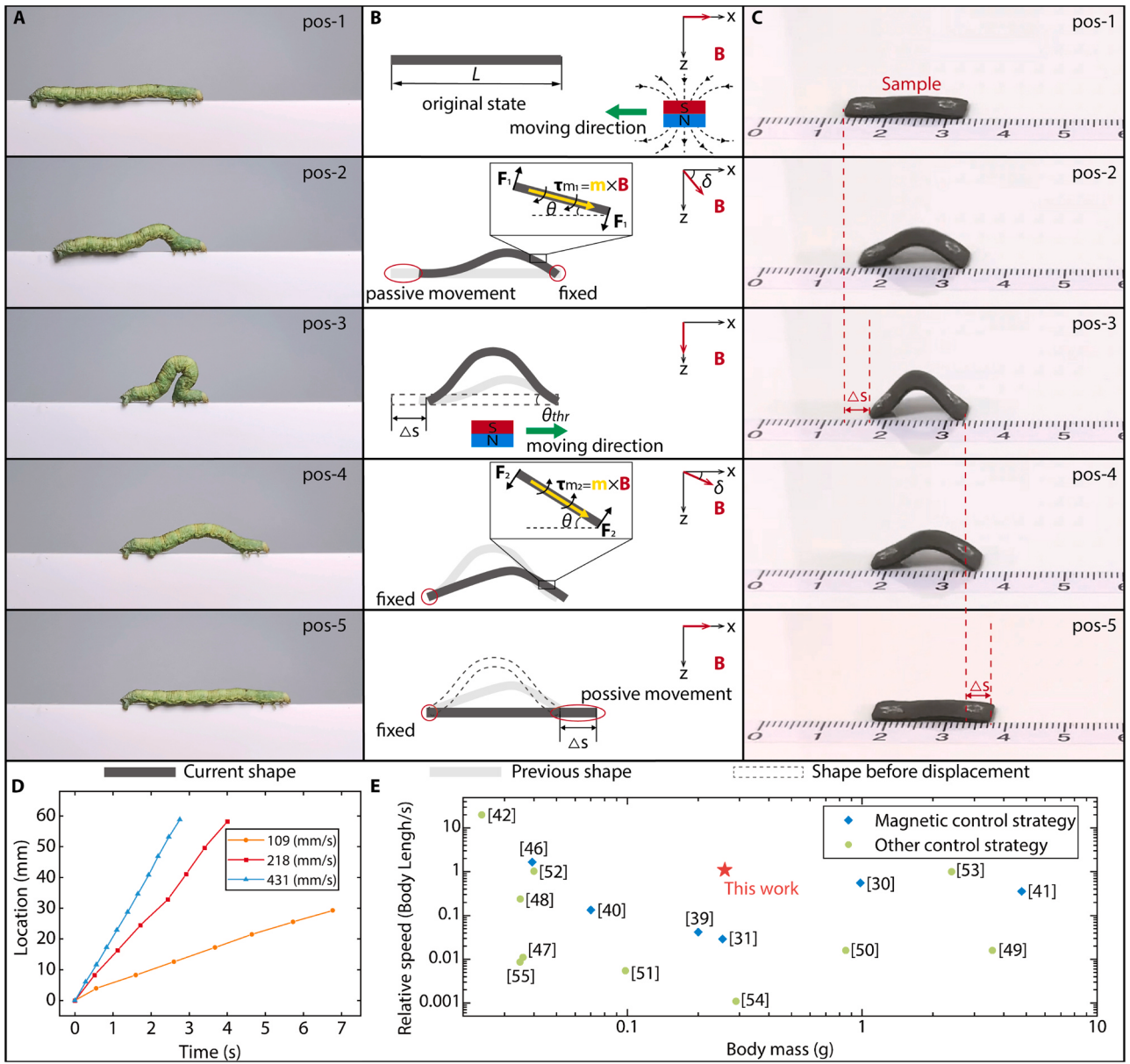


Fig. 3. Inchworm-inspired magnetic soft robot. (A) Moving posture diagram of an inchworm during a crawling cycle (see Movie S3). (B) Schematic of the motion decomposition of the magnetic soft robot. Pos-1 to pos-5 represent the morphological characteristics of the robot in different positions during a motion cycle. The red arrow represents approximately the direction of the actuating magnetic field in the robot region, and the yellow arrow represents the direction of the internal magnetic moment of the robot. (C) Photograph of the motion decomposition of the magnetic soft robot. (D) Locations of the soft robot in locomotion experiments, where 109 mm/s, 218 mm/s and 431 mm/s represent the speed of the permanent magnet. (E) Comparison of locomotion speeds of different soft robots, where relative speeds of soft robots with different body mass are provided (detailed data in Table S2). The numbers [30,31,39–42,46–55] in (E) correspond to the reference numbers, which are used to indicate the corresponding robots.

magnetic field is applied, a goldfish weighing 1.4 g (approximately 57 mm in length) swims away and drags the soft robot into the water easily. However, when a 15-mT uniform magnetic field is applied, the left side of the robot starts to deform like lifting a fishing pole. The fish tries hard to unhook, but the right part of the soft robot remains motionless, further demonstrating the effect of blank holding (see Movie S2).

Supplementary material related to this article can be found online at doi:10.1016/j.nanoen.2021.106169.

2.3. Inchworm-inspired magnetic soft robot

Soft crawling robots inspired by nature have recently aroused great interest since biological creatures exhibit a variety of smart motion patterns and strong interactions with uncertain and complex environments [36]. Among them, the inchworm-inspired robot has been widely studied owing to its simple and flexible body as well as its well-known crawling mechanism [9,10,37–41]. Currently, improving actuation performance and simplifying the manufacturing process in this field are still challenging. In this work, to demonstrate the potential application of the proposed reconfigurable and controllable magnetization method in this research area, we developed a simple-structure soft robot to achieve the crawling locomotion similar to an inchworm. A specific-designed dynamic magnetic field was proposed to asymmetrically actuate the two sides of the soft robot, which can realize the push-and-pull motion process by mimicking the inchworm (Fig. 3A). This dynamic magnetic field was generated by a cylindrical permanent magnet, with a diameter of 30 mm and a thickness of 10 mm, located at 11 mm directly below the soft robot. The permanent magnet was driven by a linear motor to achieve periodic reciprocating locomotion (Fig. S5).

Specifically, when the relatively distance between the small magnet (at the right bottom of the soft robot) and the soft robot is long, the magnet makes little difference on the internal magnetization direction of magnetic robot and no obvious deformation in the soft robot is observed (Fig. 3B, pos-1). When the magnet moves towards the soft robot (pos-2), right side of the soft robot begins to arch, while the right end is fixed, and thus the left side moves to the right, just like the inchworm (body pulling motion) in Fig. 3A. The qualitative explanation is as follows. For a given element of the robot's right side, as the actuating magnetic field increases and an angle ($\delta-\theta$) between the magnetic field direction and the magnetization direction occurs, the element tends to align towards the magnetic field direction under the action of a magnetic torque τ_{m1} with a clockwise direction. In this case, the equivalent force F_1 of the magnetic torque acts vertically on both sides of the element, exerting a downward pressure on the right end of the robot, thus increasing the static friction of the contact point with the substrate and fixing its position. For the left part of the soft robot, the generated magnetic torque is small, due to the weak magnetic field, and its rightward movement is induced mainly by the drag effect of the deformation developing on the right side. When the magnet moves to pos-3, the actuating magnetic field at the central region of the soft robot is approximately equivalent to -90° . At this moment, the left and right magnetic responses of the soft robot are symmetrical and the body pulling movement process with a displacement of Δs is complete (Fig. 3B). As the permanent magnet moves back to the right (pos-4), the angle θ between the internal magnetic moment of the robot and the horizontal direction grows larger than that of the external magnetic field, which causes the development of the counter-clockwise magnetic torque τ_{m2} . Subsequently, the equivalent force F_2 of the magnetic torque τ_{m2} exerts an upward thrust on the right end of the robot, reducing the corresponding static friction and lifting up the right end. Then the whole body starts to flatten and positive displacement along the x-axis is achieved. Finally, as the magnet eventually moves far away, the robot returns to its initial flat state. Based on the process described above, the crawling direction of the soft robot can be easily controlled, by altering the motion direction of the permanent magnet with the aid of a linear motor, thereby achieving a continuous

two-way crawling locomotion (Movie S3).

Supplementary material related to this article can be found online at doi:10.1016/j.nanoen.2021.106169.

The location of the soft robot as a function of time and under different permanent magnet actuation speeds is given in Fig. 3D. The results show that the locomotion speed of the soft robot increases as the actuation speed of the permanent magnet increases, with the maximum locomotion speed reaching about 1.1 BL/s (BL: body length, 22 mm/s) in the tests. The locomotion speed is a commonly used performance evaluation index of soft robots. A comparative summary of locomotion speeds of different soft robots from literature is provided in Fig. 3E. Considering that the weight of soft robots is influencing their locomotion speed considerably [42], taking the weight of our robot as a reference, soft robots within the range of 20 times larger and 20 times smaller (which is considered as the same weight level in this work) are sorted out for comparison. It can be seen that the speed of our soft robot is at a high level (top-3) among robots in Fig. 3E.

2.4. Multi-arm magnetic soft robot for object transportation

In this section, we show another soft robot for object transport with potential practical application in complex and unstructured environments. The soft robot was programmed to have a radial magnetization profile along its six arms, as shown in Fig. 4A. Although the soft robot has multiple arms, it only needs one step to complete its magnetization (within milliseconds), showing great potential in the high-efficiency production of such robots.

To demonstrate the functionality and performance of the soft robot, we designed a multi-configuration testing platform that consisted of a 4 mm high obstacle, a 16° slope, a right-angle turn, a U-turn and an S-shaped glass tube (Fig. 4A). The soft robot first lies prone on the ground with a cylindrical pill placed on its back (Fig. 4B). When an actuating field along the z-axis is applied, the robot folds its six arms. As the magnetic field rotates to the x-axis, the robot tilts its arms towards the field direction until three arms touch the ground. As the field direction turns from the negative z-axis to negative x-axis, the robot stands upside down and somersaults forward, holding the pill inside. This locomotion is enabled by a relatively high rotating magnetic field (about 80 mT) generated by a permanent magnet, which allows the soft robot to grasp the pill tight enough. Controlled rolling locomotion of the soft robot on the platform was achieved by continuously changing the magnetic field direction (Movie S4). To better demonstrate the motion of the robot during the transport process, we used the vector graphics software Adobe Illustrator to create composite pictures shown in Fig. 4C–F. Postures of the same robot at different moments were extracted from their original photos and superimposed onto the same background photo while keeping their relative positions on the testing platform unchanged. The flexible movement demonstrated in these complex environments is enabled by the simplicity of the steering of the soft robot, under magnetic fields. Since the soft robot tends to deform and align its arms with the field direction, we can alter the direction of B_{xy} to steer the robot along a desired direction (Fig. 4G, and Movie S5). In short, the motion mechanism of our six-arm soft robot is to achieve forward rolling under a rotating magnetic field in the x-z plane (Fig. 4B) and controlled steering under a magnetic field in the x-y plane (Fig. 4G).

Supplementary material related to this article can be found online at doi:10.1016/j.nanoen.2021.106169.

3. Conclusion

To summarize, we developed a direct magnetization method based on magnetic field focusing technology, where the local magnetization distribution can be programmed flexibly and reconfigurably within milliseconds and millimeter-scale resolution. The magnetization process of soft magnetic composites is inherently decoupled from their fabrication process, which implies that after fabrication, the magnetization



Fig. 4. Magnetic soft robot with a six-arm configuration for object transport. (A) Illustration of the testing platform for object transport. Yellow arrows represent the magnetization direction of magnetic soft robot. (B) Side view images of the rolling locomotion of the soft robot when transporting a pill under an 80-mT rotating B_{xz} generated by a permanent magnet. (C) Climbing over a 4-mm high obstacle. (D) Climbing up and down a 16° slope. (E) Making a right-angle turn and a U-turn. (F) Crossing an S-shaped glass tube with an inner diameter of 17.7 mm. (G) Top view images of the robot folding in half under an 80-mT B_{xy} aligned along different field directions. θ is a clockwise angle from the x-axis for describing the direction of B_{xz} and B_{xy} . Only one soft robot was used in these tests and images of the same robot at different times were superimposed into one image in (C)-(F) to better show the motion of the robot during the transport process. Scale bar: 10 mm.

could still be programmed flexibly by re-magnetizing, demagnetizing, multi-directional magnetizing, etc. Importantly, each magnetization step for magnetic orientation is completed synchronously with the particle magnetization process, and no additional magnetic field is needed to re-orient the magnetized particles. Furthermore, using the magnetization method and new explored actuation strategies, we developed multifunctional soft robots for performing different tasks. Compared with the existing magnetic soft robots, these robots show unique features. For instance, the developed fishing robot realizes the cooperation of local static and dynamic motion modes by combining magnetization components parallel to and perpendicular to the applied magnetic field. The inchworm-inspired crawling robot has the simplest structure and the fastest locomotion speed in comparison to other inchworm-like magnetic soft robots [31,39–41]. The six-arm robot carrying a pill features multiple capabilities with simple control such as, climbing over an obstacle, climbing up and down a slope, turning towards any two-dimensional direction and passing through an S-shaped glass tube. The special magnetization of the six-arm robot does not require multiple magnetization steps like other existing programmable magnetization methods [33–35], which can be completed in only one

magnetization step in this work. Overall, this work clearly demonstrate the high flexibility and functionality of developed magnetization method for magnetic soft materials, and could be of significance to the functional development of future robots, including, but not limited to grippers [2], bionic robots [3], and wearable flexible actuators [43,44].

4. Material and methods

4.1. Preparation of samples

Isotropic bonded NdFeB magnetic particles with a mean diameter of 5 μm (LW-BA (16–7A), Xinnuode, Ltd) were used in the experiments, with a relatively high remanence that guaranteed a stable and reliable response under magnetic actuation. Soft silicone rubber (Ecoflex 00–10, Smooth-On, Inc.) was applied as the encapsulating carrier, due to its excellent mechanical properties that can ensure the rapid deformation and recovery of the soft robot. The hard magnetic powder and silicone rubber were sufficiently mixed in a container at a 1:1 mass ratio. The homogeneous magnetic slurry was poured into molds with different shapes made of polytetrafluoroethylene and was cured at room

temperature for four hours. Ultimately, the precursors of magnetic composites containing randomly arranged and unmagnetized particles were obtained after demolding. In addition, some magnetic soft robots with different shapes can also be fabricated using the same mold and one-step magnetization way. This is undoubtedly beneficial for simplifying the total fabrication process of magnetic soft robots and enhancing mass production efficiency in practical applications. Specifically, as schematically shown in Fig. S6A, the NdFeB magnetic particles and Ecoflex 00–10 were mixed and poured into a circular mold for batch molding. Then demolded soft robots were magnetized by the developed dual-coil system. After magnetization, the samples manufactured in the same batch were cut along the red dotted line for secondary processing by a laser machine (DirectLaser S2 from Dezhong Technology Development Co., Ltd., Tianjin, China). After cutting, the soft robots with various shapes including strip, ring, three-arm plane and eight-arm plane were obtained (Fig. S6B).

4.2. Electromagnetic coil system for actuation

The uniform magnetic fields applied in Figs. 1–2 were generated using a Helmholtz coil (Fig. S7). A pair of coils powered by a Direct Current source (N5741A, 6 V/100 A, 600 W, Agilent Technologies) can realize the required constant and stable magnetic field by regulating the voltage and current amplitude. The system is able to generate a 99% homogeneous magnetic field, up to 15 mT in a spherical region with a diameter of 50 mm.

4.3. Models for electromagnetic analysis

Using the COMSOL Multiphysics Software (V5.4), two physical models including “Global ODEs and DAEs” and “magnetic fields” were established to achieve the sequential coupling of the discharge circuit and the electromagnetic field. The equivalent circuit model and the used parameters are shown in Fig. S8 and Table S1. The detailed descriptions can refer to Text S2 (circuit model) and Text S3 (electromagnetic field model). To improve the calculation speed while ensuring the accuracy, the field shaper was set as a single-turn coil with a cross-sectional current of zero, which simplified the whole structure to a 2D axisymmetric model (Fig. S9). The calculated and measured current waveforms are presented in Fig. S4, which shows a good agreement.

4.4. Models for predicting the robot deformation

The deformation analysis of soft robots under static magnetic fields was carried out using the ABAQUS/Standard package, combined with a user-defined element subroutine.[27,33] The gravity, friction, contact force and the magnetic torque were included in the finite element models. The F-bar method [45] was adopted in the simulations to avoid spurious locking and assured that large strain analysis of nearly incompressible solids could be completed. All simulations adopted the neo-Hookean material model. Magnetization, Young’s modulus and Poisson’s ratio of the soft robots were set to 61.3 kA/m, 84.5 kPa and 0.495, respectively. Friction factor between the plane and soft robots was set to 0.5. The distribution of magnetic moment density in soft robots was discretized and simplified, the magnetic moment density was assumed to be the same in a certain part and there was no transition zone between two parts with different magnetic moment densities, which brought little difference in most conditions.

Ethical approval

The procedures for care and use of animals were approved by the Institutional Animal Care and Use Committee of Tongji Medical College, Huazhong University of Science and Technology (Number: S2401).

Author contributions

All authors contributed to the writing and discussions of the manuscript. Q.L. Cao proposed, designed and directed the research. Y. Ju and Y. Xie carried out the experiments and image data processing. R. Hu carried out the review & editing. J. Yao performed the simulations of deformation of magnetic soft robots. L. Li directed and supervised the work.

Declaration of Competing Interest

The authors declare that they have no known competing financial interests or personal relationships that could have appeared to influence the work reported in this paper.

Acknowledgements

This work was supported by the National Natural Science Foundation of China (51821005), and the Young Elite Scientists Sponsorship Program by China Association for Science and Technology (YES, 2018QNRC001).

Appendix A. Supporting information

Supplementary data associated with this article can be found in the online version at doi:10.1016/j.nanoen.2021.106169.

References

- [1] M. Cianchetti, C. Laschi, A. Menciassi, P. Dario, Biomedical applications of soft robotics, *Nat. Rev. Mater.* 3 (2018) 143–153.
- [2] J. Shintake, V. Cacucciolo, D. Floreano, H. Shea, Soft robotic grippers, *Adv. Mater.* 30 (2018), 1707035.
- [3] S. Li, H. Bai, R.F. Shepherd, H. Zhao, Bio-inspired design and additive manufacturing of soft materials, machines, robots, and haptic interfaces, *Angew. Chem. Int. Ed.* 58 (2019) 11182–11204.
- [4] S. Liu, Y. Li, W. Guo, X. Huang, L. Xu, Y.C. Lai, C. Zhang, H. Wu, Triboelectric nanogenerators enabled sensing and actuation for robotics, *Nano Energy* 65 (2019), 104005.
- [5] T.J. Wallin, J. Pikul, R.F. Shepherd, 3D printing of soft robotic systems, *Nat. Rev. Mater.* 3 (2018) 84–100.
- [6] W. Hu, G.Z. Lum, M. Mastrangeli, M. Sitti, Small-scale soft-bodied robot with multimodal locomotion, *Nature* 554 (2018) 81–85.
- [7] C. Ahn, X. Liang, S. Cai, Bioinspired design of light-powered crawling, squeezing, and jumping untethered soft robot, *Adv. Mater. Technol.* 4 (2019), 1900185.
- [8] L. Wang, Z. Wang, Mechanoreception for soft robots via intuitive body cues, *Soft Robot.* 7 (2020) 198–217.
- [9] J. Cao, W. Liang, Y. Wang, H.P. Lee, J. Zhu, Q. Ren, Control of a soft inchworm robot with environment adaptation, *IEEE Trans. Ind. Electron.* 67 (2019) 3809–3818.
- [10] B. Zhang, Y. Fan, P. Yang, T. Cao, H. Liao, Worm-like soft robot for complicated tubular environments, *Soft Robot.* 6 (2019) 399–413.
- [11] M.A. Robertson, J. Paik, New soft robots really suck: vacuum-powered systems empower diverse capabilities, *Sci. Robot.* 2 (2017) eaan6357.
- [12] Z. Jiao, C. Ji, J. Zou, H. Yang, M. Pan, Vacuum-powered soft pneumatic twisting actuators to empower new capabilities for soft robots, *Adv. Mater. Technol.* 4 (2019), 1800429.
- [13] G. Gu, J. Zou, R. Zhao, X. Zhao, X. Zhu, Soft wall-climbing robots, *Sci. Robot.* 3 (2018) eaat2874.
- [14] M. Weng, Y. Duan, P. Zhou, F. Huang, W. Zhang, L. Chen, Electric-fish-inspired actuator with integrated energy-storage function, *Nano Energy* 68 (2020), 104365.
- [15] M. Zhu, M. Xie, X. Lu, S. Okada, S. Kawamura, A soft robotic finger with self-powered triboelectric curvature sensor based on multi-material 3D printing, *Nano Energy* 73 (2020), 104772.
- [16] H. Song, H. Lee, J. Lee, J.K. Choe, J. Kim, Reprogrammable ferromagnetic domains for reconfigurable soft magnetic actuators, *Nano Lett.* 20 (7) (2020) 5185–5192.
- [17] Y. Kim, G.A. Parada, S. Liu, X. Zhao, Ferromagnetic soft continuum robots, *Sci. Robot.* 4 (2019) eaax7329.
- [18] Q. Ze, X. Kuang, S. Wu, J. Wong, S.M. Montgomery, R. Zhang, J.M. Kovitz, F. Yang, H.J. Qi, R. Zhao, Magnetic shape memory polymers with integrated multifunctional shape manipulation, *Adv. Mater.* 32 (2020), 1906657.
- [19] X. Wang, G. Mao, J. Ge, M. Drack, G.S.C. Bermúdez, D. Wirthl, R. Illing, T. Kosub, L. Bischoff, C. Wang, Untethered and ultrafast soft-bodied robots, *Commun. Mater.* 1 (2020) 67.
- [20] J. Cui, T.-Y. Huang, Z. Luo, P. Testa, H. Gu, X.-Z. Chen, B.J. Nelson, L. J. Heyderman, Nanomagnetic encoding of shape-morphing micromachines, *Nature* 575 (2019) 164–168.

- [21] X. Yang, W. Shang, H. Lu, Y. Liu, R. Tan, X. Wu, Y. Shen, An agglutinate magnetic spray transforms inanimate objects into millirobots for biomedical applications, *Sci. Robot.* 5 (2020) eabc8191.
- [22] M.P. da Cunha, S. Amberg, M.G. Debije, E.F. Homburg, J.M. den Toonder, A.P. Schenning, A. Soft, A soft transporter robot fueled by light, *Adv. Sci.* 7 (2020), 1902842.
- [23] M.P. da Cunha, M.G. Debije, A.P. Schenning, Bioinspired light-driven soft robots based on liquid crystal polymers, *Chem. Soc. Rev.* 49 (2020) 6568–6578.
- [24] X.-Z. Chen, M. Hoop, F. Mushtaq, E. Siringil, C. Hu, B.J. Nelson, S. Pané, Recent developments in magnetically driven micro-and nanorobots, *Appl. Mater. Today* 9 (2017) 37–48.
- [25] Q. Cao, Q. Fan, Q. Chen, C. Liu, X. Han, L. Li, Recent advances in manipulation of micro-and nano-objects with magnetic fields at small scales, *Mater. Horiz.* 7 (2020) 638–666.
- [26] X. Zhao, Y. Kim, Soft microbots programmed by nanomagnets, *Nature* 575 (2019) 58–59.
- [27] R. Zhao, Y. Kim, S.A. Chester, P. Sharma, X. Zhao, Mechanics of hard-magnetic soft materials, *J. Mech. Phys. Solids* 124 (2019) 244–263.
- [28] E. Diller, M. Sitti, Three-dimensional programmable assembly by untethered robotic micro-grippers, *Adv. Funct. Mater.* 24 (2014) 4397–4404.
- [29] J. Zhang, O. Onaizah, K. Middleton, L. You, E. Diller, Reliable grasping of three-dimensional untethered mobile magnetic microgripper for autonomous pick-and-place, *IEEE Robot. Autom. Lett.* 2 (2017) 835–840.
- [30] S. Wu, Q. Ze, R. Zhang, N. Hu, Y. Cheng, F. Yang, R. Zhao, Symmetry-breaking actuation mechanism for soft robotics and active metamaterials, *ACS Appl. Mater. Interfaces* 11 (2019) 41649–41658.
- [31] V.K. Venkiteswaran, L.F.P. Samaniego, J. Sikorski, S. Misra, Bio-inspired terrestrial motion of magnetic soft millirobots, *IEEE Robot. Autom. Lett.* 4 (2019) 1753–1759.
- [32] L. Manamanchaiyaporn, T. Xu, X. Wu, Magnetic soft robot with the triangular head-tail morphology inspired by lateral undulation, *IEEE/ASME Trans. Mechatron.* 25 (2020) 2688–2699, <https://doi.org/10.1109/TMECH.2020.2988718>.
- [33] Y. Kim, H. Yuk, R. Zhao, S.A. Chester, X. Zhao, Printing ferromagnetic domains for untethered fast-transforming soft materials, *Nature* 558 (2018) 274–279.
- [34] T. Xu, J. Zhang, M. Salehizadeh, O. Onaizah, E. Diller, Millimeter-scale flexible robots with programmable three-dimensional magnetization and motions, *Sci. Robot.* 4 (2019) eaav4494.
- [35] Y. Alapan, A.C. Karacakol, S.N. Guzelhan, I. Isik, M. Sitti, Reprogrammable shape morphing of magnetic soft machines, *Sci. Adv.* 6 (2020) eabc6414.
- [36] S. Chen, Y. Cao, M. Sarparast, H. Yuan, L. Dong, X. Tan, C. Cao, Soft crawling robots: design, actuation, and locomotion, *Adv. Mater. Technol.* 5 (2020), 1900837.
- [37] W. Wang, J.-Y. Lee, H. Rodrigue, S.-H. Song, W.-S. Chu, S.-H. Ahn, Locomotion of inchworm-inspired robot made of smart soft composite (SSC), *Bioinspir. Biomim.* 9 (2014), 046006.
- [38] Y. Yang, D. Li, Y. Shen, Inchworm-inspired soft robot with light-actuated locomotion, *IEEE Robot. Autom. Lett.* 4 (2019) 1647–1652.
- [39] E.B. Joyee, Y. Pan, A fully three-dimensional printed inchworm-inspired soft robot with magnetic actuation, *Soft Robot.* 6 (2019) 333–345.
- [40] S. Ijaz, H. Li, M.C. Hoang, C.-S. Kim, D. Bang, E. Choi, J.-O. Park, Magnetically actuated miniature walking soft robot based on chained magnetic microparticles-embedded elastomer, *Sens. Actuators A* 301 (2020), 111707.
- [41] H. Niu, R. Feng, Y. Xie, B. Jiang, Y. Sheng, Y. Yu, H. Baoyin, X. Zeng, MagWorm: a biomimetic magnet embedded worm-like soft robot, *Soft Robot.* (2020), <https://doi.org/10.1089/soro.2019.0167>.
- [42] Y. Wu, J.K. Yim, J. Liang, Z. Shao, M. Qi, J. Zhong, Z. Luo, X. Yan, M. Zhang, X. Wang, R.S. Fearing, R.J. Full, L. Lin, Insect-scale fast moving and ultrarobust soft robot, *Sci. Robot.* 4 (2019) eaax1594.
- [43] W. Honda, S. Harada, T. Arie, S. Akita, K. Takei, Flexible electronics: wearable, human-interactive, health-monitoring, wireless devices fabricated by macroscale printing techniques, *Adv. Funct. Mater.* 24 (2014) 3298.
- [44] S. Huang, Y. Liu, Y. Zhao, Z. Ren, C.F. Guo, Flexible electronics: stretchable electrodes and their future, *Adv. Funct. Mater.* 29 (2019), 1805924.
- [45] E.A. de Souza Neto, D. Perić, M. Dutko, D.R.J. Owen, Design of simple low order finite elements for large strain analysis of nearly incompressible solids, *Int. J. Solids Struct.* 33 (1996) 3277–3296.
- [46] H. Lu, M. Zhang, Y. Yang, Q. Huang, T. Fukuda, Z. Wang, Y. Shen, A bioinspired multilegged soft millirobot that functions in both dry and wet conditions, *Nat. Commun.* 9 (2018) 3944.
- [47] Y. Ma, Y. Zhang, B. Wu, W. Sun, Z. Li, J. Sun, Polyelectrolyte multilayer films for building energetic walking devices, *Angew. Chem.* 123 (2011) 6378–6381.
- [48] B. Shin, J. Ha, M. Lee, K. Park, G.H. Park, T.H. Choi, K.-J. Cho, H.-Y. Kim, Hygrobot: a self-locomotive ratcheted actuator powered by environmental humidity, *Sci. Robot.* 3 (2018) eaar2629.
- [49] N. Tomita, K. Takagi, K. Asaka, Development of a quadruped soft robot with fully IPMC body, *SICE Annual Conference 2011*, pp. 1687–1690, 2011.
- [50] I. Must, F. Kaasik, I. Pöldsalu, L. Mihkel, U. Johanson, A. Punning, A. Aabloo, Ionic and capacitive artificial muscle for biomimetic soft robotics, *Adv. Eng. Mater.* 17 (2015) 84–94.
- [51] D. Morales, E. Palleau, M.D. Dickey, O.D. Velev, Electro-actuated hydrogel walkers with dual responsive legs, *Soft Matter* 10 (2014) 1337–1348.
- [52] M. Duduta, D.R. Clarke, R.J. Wood, A high speed soft robot based on dielectric elastomer actuators, *2017 IEEE International Conference on Robotics and Automation (ICRA)*, pp. 4346–4351, 2017.
- [53] A.M. Hoover, E. Steltz, R.S. Fearing, RoACH: An autonomous 2.4g crawling hexapod robot, *2008 IEEE/RSJ International Conference on Intelligent Robots and Systems*, pp. 26–33, 2008.
- [54] C. Wang, K. Sim, J. Chen, H. Kim, Z. Rao, Y. Li, W. Chen, J. Song, R. Verduzco, C. Yu, Soft ultrathin electronics innervated adaptive fully soft robots, *Adv. Mater.* 30 (2018), 1706695.
- [55] Y.Y. Xiao, Z.C. Jiang, X. Tong, Y. Zhao, Biomimetic locomotion of electrically powered “Janus” soft robots using a liquid crystal polymer, *Adv. Mater.* 31 (2019), 1903452.



Yuwei Ju received her B.S. degree from the School of Electrical and Electronics Engineering (SEE) at Huazhong University of Science and Technology (HUST) in 2018, Wuhan, China. Currently, she is pursuing her Ph.D. degree under the supervision of Prof. Liang Li at Wuhan National High Magnetic Field Center (WHMFC), HUST. Her research interests focus on magnetic soft robotics, biomimetic robots and pulsed high magnetic field technology.



Run Hu is an Associate Professor in the School of Energy and Power Engineering at Huazhong University of Science and Technology (HUST), Wuhan, China. He received his B.S. in Thermal Power Engineering at HUST in 2010, and Ph.D. in Engineering Thermophysics at HUST in 2015. He visited Purdue University, West Lafayette, IN, US in 2015 spring. He was a JSPS postdoctoral fellow of Department of Mechanical Engineering at The University of Tokyo from 2016 to 2017. His research interests include thermal functional materials and devices and thermal management of electronics.



Yan Xie received his B.S. degree from the School of Electrical and Electronics Engineering (SEE) at Huazhong University of Science and Technology (HUST) in 2019, Wuhan, China. He is currently pursuing his M.S. degree at Wuhan National High Magnetic Field Center (WHMFC), HUST. His research interests include soft robot for medical applications and pulsed high magnetic field technology.



Jianpeng Yao received his B.S. degree from the School of Electrical and Electronics Engineering (SEE) at Huazhong University of Science and Technology (HUST) in 2019, Wuhan, China. He is currently pursuing his M.S. degree at Wuhan National High Magnetic Field Center (WHMFC), HUST. His research interests include magnetic soft robotics and machine learning.



Xiaoxiang Li is a postdoctor in the School of Materials Science and Engineering at Huazhong University of Science and Technology (HUST), Wuhan, China. He received his B.S. degree in Electrical Engineering and Its Automation at Wuhan University of Technology (WHUT) in 2015, and Ph.D. degree in Electrical Engineering at HUST in 2020. His research interests include magnetic pulse welding, electromagnetic forming and applications of high magnetic field.



Quanliang Cao is an Associate Professor in the Wuhan National High Magnetic Field Center (WHMFC) and the School of Electrical and Electronics Engineering (SEEE) at Huazhong University of Science and Technology (HUST), Wuhan, China. He received his B.S. and Ph.D. degrees from the SEEE at HUST in 2008 and 2013, respectively. His research interests focus on the magnetic field technology and its applications, including magnetic soft robotics, magnetic separation and electromagnetic forming.



Yiliang Lv is an Associate Professor in the Wuhan National High Magnetic Field Center (WHMFC) and the School of Electrical and Electronics Engineering (SEEE) at Huazhong University of Science and Technology (HUST), Wuhan, China. He received his B.S. and Ph.D. degrees from the SEEE at HUST in 2007 and 2013, respectively. His research interests focus on the generation and application of high magnetic field, including post-assembly magnetization of permanent magnet motors and permanent magnet materials.



Liang Li is a Professor in the Wuhan National High Magnetic Field Center (WHMFC) and the School of Electrical and Electronics Engineering (SEEE) at Huazhong University of Science and Technology (HUST), Wuhan, China. He is the director of the WHMFC. He received his Ph.D. degree from Katholieke Universiteit Leuven (K.U. Leuven), Belgium, in 1997. His research interests cover the development of high field pulsed magnets, superconducting magnets, fusion magnets and their applications.



Xiaotao Han is a Professor in the Wuhan National High Magnetic Field Center (WHMFC) and the School of Electrical and Electronics Engineering (SEEE) at Huazhong University of Science and Technology (HUST), Wuhan, China. He received his Ph.D. degree from the SEEE at HUST in 2004. His research interests focus on the application of high magnetic field such as electromagnetic forming, magnetic separation, and bioelectromagnetics.